

Journal Pre-proof

Development of an impedimetric immunosensor to determine microcystin-LR. New approaches in the use of The electrochemical impedance spectroscopy was used in determining to determine kinetic parameters of immunoreactions

Micaela Boffadossia, Aylen Di Toccoa, Gabriel Lassabec, Macarena Pérez-Schirmerc, Sebastián Noel Robledo, Héctor Fernández, María Alicia Zon, Gualberto González-Sapienza, Fernando Javier Arévalo

PII: S0013-4686(20)31014-8

DOI: <https://doi.org/10.1016/j.electacta.2020.136621>

Reference: EA 136621

To appear in: *Electrochimica Acta*

Received Date: 20 April 2020

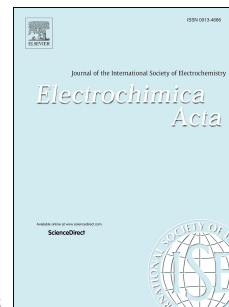
Revised Date: 29 May 2020

Accepted Date: 10 June 2020

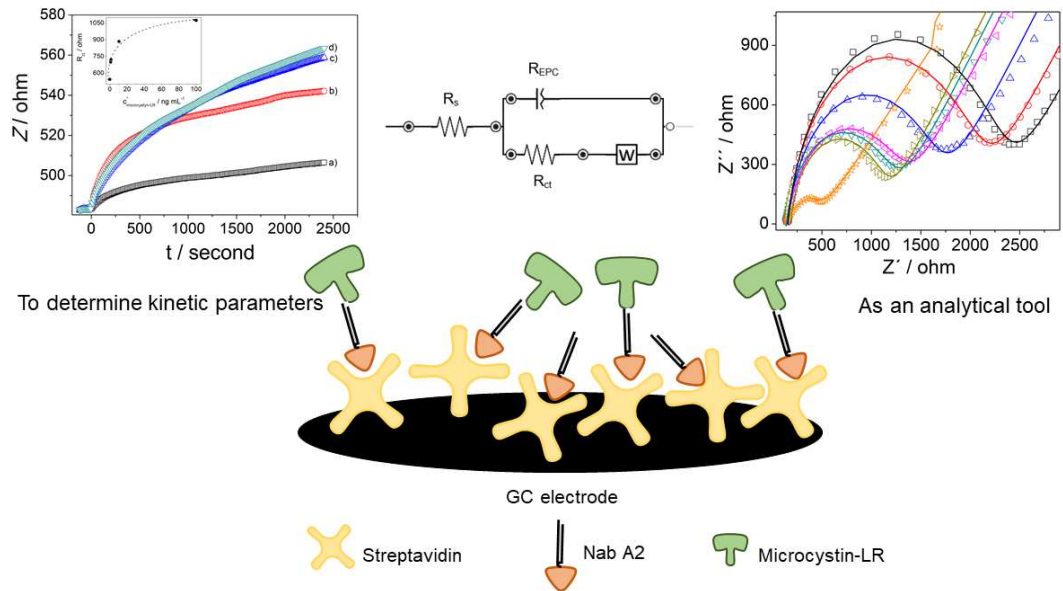
Please cite this article as: M. Boffadossia, A. Di Toccoa, G. Lassabec, M. Pérez-Schirmerc, S.N. Robledo, H. Fernández, M.A. Zon, G. González-Sapienza, F.J. Arévalo, Development of an impedimetric immunosensor to determine microcystin-LR. New approaches in the use of The electrochemical impedance spectroscopy was used in determining to determine kinetic parameters of immunoreactions *Electrochimica Acta*, <https://doi.org/10.1016/j.electacta.2020.136621>.

This is a PDF file of an article that has undergone enhancements after acceptance, such as the addition of a cover page and metadata, and formatting for readability, but it is not yet the definitive version of record. This version will undergo additional copyediting, typesetting and review before it is published in its final form, but we are providing this version to give early visibility of the article. Please note that, during the production process, errors may be discovered which could affect the content, and all legal disclaimers that apply to the journal pertain.

© 2020 Elsevier Ltd. All rights reserved.



Graphical abstract



Development of an impedimetric immunosensor to determine microcystin-LR. ~~New approaches in the use of~~ The electrochemical impedance spectroscopy was used in ~~determining~~ to determine kinetic parameters of immunoreactions

Micaela Boffadossi^a, Aylén Di Tocco^a, Gabriel Lassabe^c, Macarena Pírez-Schirmer^c, Sebastián Noel Robledo^b, Héctor Fernández^a, María Alicia Zon^a, Gualberto González-Sapienza^{c,*}, Fernando Javier Arévalo^{a,*}

^aGrupo de Electroanalítica (GEANA), Departamento de Química, Facultad de Ciencias Exactas, Físicoquímicas y Naturales, Universidad Nacional de Río Cuarto. Instituto para el Desarrollo Agroindustrial y de la Salud (IDAS, CONICET-UNRC), Agencia Postal No. 3 (5800), Río Cuarto, Argentina.

^bGrupo de Electroanalítica (GEANA), Departamento de Tecnología Química, Facultad de Ingeniería, Universidad Nacional de Río Cuarto. Instituto para el Desarrollo Agroindustrial y de la Salud (IDAS, CONICET-UNRC). Agencia Postal No. 3, 5800 Río Cuarto, Argentina.

^cCátedra de Inmunología, Facultad de Química, Instituto de Higiene, UDELAR, Av. A. Navarro 3051, Piso 2, Montevideo, 11600, Uruguay

E-mail addresses: farevalo@exa.unrc.edu.ar, fernandojavierarevalo@gmail.com,

Tel.: +54 0358 4676 111 (F. J. Arévalo); ggonzal@fq.edu.uy (G. González-Sapienza)

Abstract

The development of new electrochemical immunosensors for the detection of environmental contaminants is of great interest due to their simplicity, high sensitivity, and extended analytical range. Because of the antibody is immobilized on the electrode, it is important to determine its loss of reactivity after immobilization. In this work, two aspects were addressed. First, we developed a new methodology based on electrochemical impedance (EI) to determine the kinetic parameters associated with immunoreactions carried out on the electrode. Second, an electrochemical immunosensor based on electrochemical impedance spectroscopy (EIE) was developed to determine microcystin-LR in drinking water samples. Microcystin-LR determination was based on a label-free non-competitive immunoassay. The electrochemical immunosensor shows a limit of detection (LOD) of 33 pg mL^{-1} ($3.32 \times 10^{-11} \text{ mol L}^{-1}$ or $0.033 \text{ } \mu\text{g L}^{-1}$) which is well below the WHO guideline recommendation of $1 \text{ } \mu\text{g L}^{-1}$ and 40 times better than the LOD obtained using the same antibody in an optimized conventional competitive ELISA assay. In addition, an acceptable accuracy, with recovery percentages close to 100% were found. The label-free immunosensor is a valuable tool to monitor microcystin-LR in drinking water samples and the environment.

Keywords: Microcystin; Determination of affinity constant by electrochemical impedance; Heterogeneous immunoassay.

1. Introduction

The development of new electrochemical immunosensors for the detection of environmental contaminants is of great interest due to their simplicity, high sensitivity, and extended analytical range. Electrochemical immunosensors are a type of biosensors, which are differentiated by the immobilization of antibodies on the electrode surface. They are powerful analytical tools due to their sensibility, portability and low-cost. Electrochemical immunosensors show a high sensitivity and an analytical extended range. They are fast, reliable and inexpensive tools to determine analytes in different samples [1].

Electrochemical immunosensors combine the selectivity of the antibodies with the sensitivity of electrochemical techniques, and are particularly suitable for the rapid and direct detection of the antibody–antigen interactions. The construction of electrochemical immunosensors requires the immobilization of the antibody on the electrode, which is the key stage that determines the stability, reproducibility and sensibility of the assay [2]. The efficient control and orientation of the immobilized antibody on the sensor surface produces an improved molecular recognition layer, optimizing the immunosensor performance. Therefore, oriented and close-packed immobilization of the antibody is critical to avoid steric hindrance around the antigen-binding site and to maximize the antigen-binding capacity. There are different ways to immobilize the antibody on the sensor surface, commonly using passive adsorption through non-specific interactions, covalent bonding via available

carboxylic, amino or thiol groups, or through interaction of the Fc region of the antibody with protein G or A modified surfaces [3,4]. Only the later provides an oriented immobilization of whole Ig molecules and assures preservation of the antigen binding site.

The sensitivity of the immunosensor depends mainly on two factors: the reactivity of the immunoreaction between the antibody and its antigen and the sensitivity of the transducer. The reactivity of the immunoreaction is characterized by the dissociation constant (K_D), which depends on the association (k_a) and dissociation (k_d) rates. K_D values between 10^{-10} - 10^{-5} nM are necessary for the development of a sensitive immunoassay [5]. It is possible that depending on the immobilization strategy the affinity of an antibody for its cognate antigen may be affected. Therefore, the determination of these thermodynamic parameters on the immobilized antibody can help us to understand and improve the performance of the immunosensor.

Electrochemical impedance spectroscopy (EIS) is an electrochemical technique used for the characterization of electrode surfaces in diverse fields as energy, electrocatalysis, medicine and analytical [6]. On the other hand, EIS is a powerful electrochemical technique for investigating electrode reactions, the kinetics of adsorption reactions on the electrode, as well as physical properties such as diffusion coefficients and chemical reaction rates. EIS measures the relationship between the current and the applied potential difference for a frequency region [7]. Potentiostatic EIS mode, a small sinusoidal wave of potential (ideally infinitesimally) is applied between the working and counter electrodes in a frequency range. Sinusoidal current or voltage are recorded, and from voltage-to-current amplitude ratio and the phase lag between input and

output, a complex function Z (impedance) is obtained, which depend on the frequency f [6-78]. This technique can be used for analytic purpose. There are hundreds of reports in the literature using EIS in the development of affinity sensors. An interesting advantage of using the EIS in the development of affinity sensor for the detection of small compound is the possibility of performing a non-competitive label-free assay. Interestingly, it also allows exploring each step of the electrode modification and determining the electrical properties of the electrode [9]. The interpretations of the results are carried out using multiple models or electrical circuits which represent the electrochemical system. Therefore, more than one model can be used and thus obtain ambiguous or erroneous results [8]. The problem is solved from the correct physical interpretation of the electrochemical system and the statistical analysis of the parameters resulting from the model used in the fit of the experimental data.

A very interesting and unexplored aspect is the use of EI for the determination of kinetic parameters of bio-reactions on the electrode surface. In EI, the electrical potential applied at the working electrode is a waveform disturbance with a constant frequency and an amplitude of a few millivolts around the equilibrium potential of the solution, which produces minimal changes at the electrode or in its proximities. This fact allows us to study in real time, for example, the reaction between an antigen and an antibody on the electrode and, determine the corresponding kinetic parameters.

In this work, these concepts are used to develop an electrochemical immunosensor to quantify microcystin-LR. Microcystins are one of the most common and hazardous cyanotoxins, with hundreds of structural variants [10].

They are produced by different species of cyanobacterias, commonly associated with blue algae blooms occurring in rivers and lakes, drinking water, etc. [11]. Microcystins are a family of hepatotoxic peptides, with a common peptide ring structure formed by 7 amino acids. Two of them are proteinogenic while the other five are not. The most common microcystin is the microcystin-LR. The term LR is due to the amino acids leucine and arginine present in the molecular structure of the microcystin [10]. Cases of severe hepatotoxicity caused by microcystin-LR have been found in both humans and animals [12]. Drinking water contaminated with microcystin-LR produces harmful effects on human health, such as carcinogenesis, skin irritation, diarrhea and liver damage. [13]. Therefore, the World Health Organization (WHO) has issued a guideline maximum level of microcystin-LR concentration in drinking water of $1 \mu\text{g L}^{-1}$ [14].

A promising alternative to the use of conventional antibodies in the development of immunoassays is the use of variable domains of heavy-chain-only antibodies (VHH). The recombinant VHH antibody fragments (nanobodies) derived from the heavy-chain only antibodies found in camelids have proved to be advantageous recombinant reagents for immunoassay [15-17]. Pérez-Schirmer et al. [18] described the construction of a VHH phage display library against microcystin-LR and the selection of high affinity nanobodies (NABs) to microcystin-LR using novel panning strategies. Each strategy was evaluated by a large-scale screening using in vivo biotinylated NABs. Thus, the VHH A2 was isolated which allowed to develop a microcystin-LR competitive ELISA that performed with excellent recovery and high sensitivity of 0.28 ng mL^{-1} in water.

In this work, two topics were studied. First, we report the use of the NAb A2 to develop a highly sensitive electrochemical immunosensor to measure microcystin-LR in drinking water. Second, using this VHH as a model antibody we present a new method to determine the K_D of immobilized ligands using EI [18]. The microcystin-LR determination was performed using the biotinylated nanobody (Nab A2) immobilized on a glassy carbon electrode that has previously been modified by an imine bond formed between streptavidin and the generated electrochemically oxygenated group on the electrode. The interaction between microcystin-LR and the NAb A2 was determined by EI (Scheme 1).

Preferred position of Scheme 1

2. Material and methods

2.1. Chemicals, antibodies and other reagents

Microcystin-LR was purchased from Enzo Life Sciences (New York, USA). The anti-microcystin-LR biotinylated nanobody (Nab A2) was obtained as described in previous report [18]. Streptavidin was from Fermentas Thermo Fisher, CA (Waltham, USA). NaOH and $\text{Fe}(\text{NH}_4)_2(\text{SO}_4)_2 \cdot 6\text{H}_2\text{O}$ were from Merck (Darmstadt, Germany), *N*-(3-dimethylaminopropyl)-*N*-(ethylcarbodiimide)-hydrochloride (EDC) and *N*-Hydroxysuccinimide (NHS) were from Sigma-Aldrich (St. Louis, USA). Bidistilled water was obtained in our laboratory and used for the preparation of a $10 \times 10^{-3} \text{ mol L}^{-1} \text{ KH}_2\text{PO}_4 + \text{Na}_2\text{HPO}_4$, $0.137 \text{ mol L}^{-1} \text{ NaCl}$ and $2.70 \times 10^{-3} \text{ mol L}^{-1} \text{ KCl}$, pH 7.0 phosphate buffer solution, pH = 7, (PBS), from its salts, all from Merck (Darmstadt, Germany). Potassium hexacyanoferrate (III) ($\text{K}_3[\text{Fe}(\text{CN})_6]$) and potassium hexacyanoferrate (II) ($\text{K}_4[\text{Fe}(\text{CN})_6]$) and KCl, p.a., were obtained from Merck (Darmstadt, Germany). 1

$\times 10^{-3} \text{ mol L}^{-1} \text{ K}_4[\text{Fe}(\text{CN})_6] + 1 \times 10^{-3} \text{ mol L}^{-1} \text{ K}_3[\text{Fe}(\text{CN})_6] + 0.1 \text{ mol L}^{-1} \text{ KCl}$ solution was prepared and was used for all measurements.

Drinking water samples were obtained by collecting from reservoirs of the Rio Cuarto city, Córdoba, Argentina, after allowing the tap water to drain during five minutes. Then, the water samples were spiked with different amounts of microcystin-LR at concentration at levels of 0.1 and 1 ng mL⁻¹. The water samples were measured by the electrochemical immunosensor without any prior treatment.

2.2. Materials and apparatus

A conventional glass cell of three electrodes was used. The volume of the solution in the cell was 2 mL. The working and reference electrodes were a glassy carbon (GC) disk (3 mm dia.) and an Ag/AgCl, respectively, both from CH Instruments, Inc. (Austin, USA). The counter electrode was a homemade Pt wire of large area ($A \approx 1 \text{ cm}^2$). Electrochemical measurements were performed using a PalmSens 4 potentiostat, Compact Electrochemical Interfaces (Houten, The Netherlands), controlled by PSTrace 5.7 software. The electrochemical impedance spectra were fitted using the PSTrace 5.7 software.

2.3. Methods

2.3.1. Preparation of electrochemical immunosensor

The GC-electrode disk was polished with alumina (0.3 and 0.05 μm diameter) and sonicated in water for two min each one before its modification. Then, the generation of oxygenated functional groups on the GC electrode was carried out by electrooxidation in 0.1 mol L⁻¹ H₂SO₄ or 0.1 mol L⁻¹ NaOH

solutions. The oxidations were performed by amperometry applying 1.2 V for 300 s. To verify the formation of superficial carboxyl groups, cyclic voltammetry was performed in $1 \times 10^{-3} \text{ mol L}^{-1} \text{ Fe}(\text{NH}_4)_2(\text{SO}_4)_2 + 0.1 \text{ mol L}^{-1} \text{ KCl}$ solution [19]. Once the carboxyl groups were generated on the electrode, it was immersed in $1 \times 10^{-4} \text{ mol L}^{-1} \text{ EDC} + 5 \times 10^{-5} \text{ mol L}^{-1} \text{ NHS}$, in PBS for 30 min. Then, the electrode was washed with PBS and allowed to react with a $100 \mu\text{g mL}^{-1}$ of streptavidin overnight at $4 \text{ }^\circ\text{C}$. Next, the streptavidin/GC electrode was washed with 0.1% BSA in PBS. Finally, the Nab A2/streptavidin/GC electrode was constructed after loading the sensor with $15 \mu\text{L}$ of $10 \mu\text{g mL}^{-1}$ Nab A2 in PBS for 45 min, followed by three washes with 0.1% BSA/PBS.

2.3.2. Electrochemical impedance measurements

A sinusoidal wave centered at the equilibrium potential of redox couple (around 75 mV) was applied in a frequency range from 50 mHz to 0.5 MHz with an amplitude of 0.015 V. A $2 \times 10^{-3} \text{ mol L}^{-1} [\text{Fe}(\text{CN})_6]^{4-/3-} + 0.1 \text{ mol L}^{-1} \text{ KCl}$ solution was used for the electrochemical impedance measurements. The electrochemical impedance spectra were fitted using a Randles circuit constructed with a solution resistance (R_s) in series with a parallel circuit formed for a constant phase element, a pseudo-capacitance (EPC) in parallel to a charge transfer resistance (R_{ct}), which is in series with a Warburg element (W) (Fig. 1) [6]. To obtain the kinetic profiles of the immunoreactions a $2 \times 10^{-3} \text{ mol L}^{-1} [\text{Fe}(\text{CN})_6]^{4-/3-} + \text{PBS}$ solution was used. The measurements of total impedance (Z) with respect to frequency were performed by applying a sinusoidal wave with a frequency of 80 Hz and an amplitude of 0.015 V during

45 min in a stirred solution at 150 rpm. All experiments were conducted at (25 ± 2) °C.

Preferred position of Fig. 1

2.3.3. Immunoassays performed with the electrochemical immunosensor

A non-competitive immunoassay was used for the detection and quantification of microcystin-LR using the electrochemical immunosensor. Initially, 25 μL of 3% BSA in PBS was added on the immunosensor for 30 min at 37 °C, in order to prevent non-specific adsorption. Then, the immunosensor was washed as described above, and 15 μL of the microcystin-LR standard solutions or water samples were added to the immunosensor and incubated at 37 °C during 45 min. The microcystin-LR/Nab A2/streptavidin/GC electrode was obtained. Then, the immunosensor was washed with PBS and introduced into the electrochemical cell containing a 2×10^{-3} mol L⁻¹ $[\text{Fe}(\text{CN})_6]^{4-/3-}$ + 0.1 mol L⁻¹ KCl solution. Finally, EIS measurements were carried out as described in Section 2.3.2.

3. Results and discussion

Immunoassays for the quantification of high molecular weight molecules can be performed in sensitive sandwich format, because their large size makes possible the simultaneous binding of two or more antibodies [5]. This is not the case for the immunodetection of small analytes, which typically require less efficient competitive methods that require the use of tracer conjugates of the analyte. In that regard, it is interesting to consider the use of highly sensitive electrochemical immunosensors. It is well known that the detection/quantification of large molecules can be performed by EIS, avoiding

the use of labeled antibodies and which could overcome these limitations allowing the direct detection and thus generating an *label-free* immunoassay [9]. In addition, EI allows us to obtain information about the kinetic parameters of the immune-reaction on the electrode, which can also help to optimized the immunosensor performance.

3.1. Preparation of electrode for the streptavidin immobilization

The streptavidin binding at the GC electrode was via an imine bond as previously described (Section 2.3.1). Initially, the massive oxidation of the CG electrode was both performed by the amperometry technique in both basic and acidic aqueous solutions. The $\text{Fe}^{2+/3+}$ couple was used to verify the carbonyl groups on the GC electrode, on the basis that the superficial carbonyl groups catalyze the electronic transfer of $\text{Fe}^{2+/3+}$ when the GC electrode is used [19]. Fig. 2 shown the cyclic voltammograms obtained for the $\text{Fe}^{2+/3+}$ redox couple after the electro-oxidation. From these results, it can be observed that the ΔE_p (difference between cathodic and anodic peak potentials) is lower when the oxidation was performed in $0.1 \text{ mol L}^{-1} \text{ NaOH}$. This can be explained considering that the electron transfer rate of the $\text{Fe}^{2+/3+}$ redox couple is higher when the oxidation is performed in basic solution, which indicates a higher density of carbonyl groups on the GC electrode after the oxidation process. In addition, the reproducibility (variation coefficient = 2.72%) was better when the oxidation was performed in a basis solution, and this condition was used throughout this study. EIS was then used to evaluate the immobilization of streptavidin. A saturation concentration of streptavidin ($100 \mu\text{g mL}^{-1}$) was allowed to react with the oxidized GC electrode as described. The R_{ct} values

obtained for both the GC electrode and streptavidin/GC electrode were 151.7 and 293.2 ohm, respectively (Fig. 3). The increase in R_{ct} is due to streptavidin binding to the electrode surface.

Preferred position of Figs. 2 and 3

3.2. Optimization of biotin-NAb concentration

In a non-competitive immunoassay, an excess concentration of capture antibodies is advantageous, because as inferred by the mass action law the formation of the immune complex is favored even in the presence of small amounts of analyte. Therefore, amount of NAb A2 immobilized on the sensor was explored using solutions in the range concentration from 2.5 to 15 $\mu\text{g mL}^{-1}$. The increase in the Nab A2 concentration produced an increment of R_{ct} of 322.4; 1265.0; 1471.2, and 1533.0 ohm, respectively (Fig. 4). The R_{ct} values for Nab A2 concentrations of 10 and 15 $\mu\text{g mL}^{-1}$ are similar, indicating the saturation of the surface. Therefore a concentration of 10 $\mu\text{g mL}^{-1}$ was chosen for the construction of the electrochemical immunosensor.

Preferred position of Fig. 4

3.3. Determination of K_D using EI

EI is a powerful electrochemical technique to investigate electrode reactions and to determine the surface-adsorption kinetics as well as mass transport parameters by applying small perturbations of the electrical potential. Therefore, EI can be used to investigate the kinetic properties of immunoreactions on the electrode surface from experiments conducted at a

fixed frequency using a redox couple as an electrochemical probe [20]. In the immunoassays, the sensitivity depends on K_D value. Low K_D values produce sensitive immunoassays, and the K_D value of an antibody could be affected by the way it is immobilized on electrode surface.

The total impedance Z , where $Z = Z' + jZ''$ (Z' and Z'' are real and imaginary components of total impedance, respectively, and $j = \sqrt{-1}$) depends on the wave frequency and may change when the concentration of adsorbed molecules on the electrode surface changes. In a steady solution (in the absence of convective forces) the Warburg term is a function of the diffusion coefficient and Z is proportional to R_{ct} (impedance of stationary systems) [21]. In a stirred solution (hydrodynamic electrochemical impedance), the solution of Z is more complex. However, Z is also proportional to R_{ct} and the Warburg impedance (diffusion parameter) has no physical meaning. Thus, the Z variation vs. time can be used for obtaining the K_D value of antigen-antibody interaction, when the frequency applied is in the highest value of R_{ct} .

The interaction of microcystin-LR immunosensor was analyzed in the range of 0.01 to 10 ng mL⁻¹. EIs were performed at a frequency = 80 Hz, corresponding to high values of R_{ct} , to generate *impedimetric sensograms* (Z vs. t) (Fig. 5). Thus, 10 μ L of a microcystin standard solution prepared in PBS was added into the electrochemical cell. Once microcystin-LR was added to the solution, an increase in Z was observed indicating the association between the toxin and the Nab A2. When a blank solution (only PBS) was added, any change was observed.

Preferred position of Fig. 5

The variation of $\ln(Z)$ was linear with the time, indicating a first-order kinetic [22]. Therefore, for each impedimetric sensogram, $\frac{\partial Z}{\partial t}$ was plotted vs. Z (Eq. 1) (Fig. 6). The slopes obtained were plotted versus the microcystin-LR concentration (Fig. 7), according to Eq. 2, where k_{as} and k_{dis} are the association and dissociation rate constants, respectively [23]:

$$\frac{\partial Z}{\partial t} [\text{ohms}^{-1}] = \text{slope} [\text{s}^{-1}] \times Z [\text{ohm}] \quad (1)$$

$$\text{slope} [\text{s}^{-1}] = k_{as} [\text{s}^{-1} \text{ mol}^{-1} \text{L}] \times C_{\text{microcystin-LR}}^* [\text{molL}^{-1}] + k_{dis} [\text{s}^{-1}] \quad (2)$$

Preferred position of Figs. 6 and 7

Values of $(1.4 \pm 0.3) \times 10^6 \text{ mol}^{-1} \text{ L s}^{-1}$ and $(2.0 \pm 0.5) \times 10^{-3} \text{ s}^{-1}$ were obtained for k_{as} and k_{dis} , respectively. The k_{as} indicates a fast association between microcystin-LR and the Nab A2. The K_D was $(1.4 \pm 0.9) \text{ nmol L}^{-1}$. These values are in good agreement with those reported by antibodies used in immunoassays [5,24]. Therefore, it seems that the affinity of the Nab A2 for the antigen was not affected by its immobilization on the electrode. The results suggest that EI could be used as an easy and inexpensive technique to determine the kinetic parameters of immuno-reactions on electrodes. On the other hand, a very important aspect is that this methodology can be applied to electrodes of different materials in the construction of immunosensors, showing a great advantage over surface plasmon resonance and quartz crystal microbalance.

3.4. Non-competitive electrochemical immunosensor for microcystin-LR quantification

The calibration curve for microcystin-LR was performed in the 1×10^{-3} to 100 ng mL^{-1} range, which is shown in Fig. 8 with the corresponding EIS spectra. There is a background signal in the absence of microcystin-LR, which is due to the R_{ct} obtained in the blank solution (see insert of Fig. 8). The calibration curve was plotted as a binding ratio (B/B_0) vs. microcystin-LR concentration, where B is the R_{ct} obtained for each microcystin-LR concentration, and B_0 is the maximum R_{ct} value obtained when the microcystin concentrations are $\geq 1 \times 10^2 \text{ ng mL}^{-1}$ (saturation concentration of immobilized antibody) and B_0 is the R_{ct} maxima, obtained when the saturation is reached. R_{ct} values were obtained by fitting each impedance spectra using the Randles circuit. The calibration curve was fitted using a four parameter-logistic equation. A limit of detection (LOD) of $3.3 \times 10^{-2} \text{ ng mL}^{-1}$ ($3.32 \times 10^{-11} \text{ mol L}^{-1}$) was obtained. The LOD was calculated as the microcystin-LR concentration which causes an increase in signal equal to three times the blank standard deviation [25]. The sensitivity (SC50) was 1.15 ng mL^{-1} . The linear range of calibration curve was from 0.1 to 10 ng mL^{-1} . These values are lower than those previously reported for this antibody [18].

Preferred position of Fig. 8

The reproducibility of the electrochemical immunosensor was checked using three standard solutions of microcystin-LR (0.1 , 1 and 10 ng mL^{-1}). These series of measurements were repeated for four consecutive days to estimate

the inter-assay values. As summarized in Table 1, the electrochemical immunosensor showed a very good reproducibility.

Preferred position for Table 1

From 2019 to date, there are more than 80 scientific papers on the development of sensors/biosensors and methodologies for the detection and quantification of microcystin-LR. Table 2 shown the latest immunosensors developed. Our electrochemical immunosensor has a competitive LOD. However, our immunosensor shows a great advantage over the simplicity of the electrochemical immunoassay. Labeling of a microcystin-LR or the use of a labeled secondary antibody is not required. Therefore, fewer reagents are needed and a shorter assay time is obtained. On the other hand, the LOD reached was 30-times lower than the limit concentration established by the WHO for microcystin-LR in drinking water [14].

Preferred position for Table 2

3.5. Microcystin-LR determination in drinking water

The matrix effect was studied using eight drinking water samples collected from four areas of the Río Cuarto city. Initial analysis showed that all samples have undetectable levels of the toxin, then, the samples were spiked with two concentration levels (0.1 and 1.0 ng mL⁻¹) of microcystin-LR (Table 3). The results obtained showed the good recoveries obtained with the electrochemical immunosensor. Therefore, this electrochemical immunosensor can be used as a good analytical tool for environmental monitoring due to its high sensitivity and extended analytical range.

Preferred position for Table 3

4. Conclusions

This work addressed two fundamental aspects. First, we developed a new methodology for monitoring, in real-time, immunoreactions on the electrode based on electrochemical impedance. This allowed to characterize the kinetics parameters of the immunoreaction between Nab A2 immobilized on the electrode surface and microcystin-LR ($K_D = (1.4 \pm 0.9) \text{ nmol L}^{-1}$, $k_{as} = (1.4 \pm 0.3) \times 10^6 \text{ mol}^{-1} \text{ L s}^{-1}$ and $k_{dis} = (2.0 \pm 0.5) \times 10^{-3} \text{ s}^{-1}$). This methodology allows the optimization of the immobilization of antibodies at the electrode and to assess possible changes in the affinity of antibodies upon immobilization, and thus to select the most suitable chemistry reaction to attach it to the sensor surface. A very important aspect is that this methodology can be applied to electrodes of different materials in the construction of immunosensors, showing a great advantage over surface plasmon resonance and quartz crystal microbalance.

Second, a sensitive electrochemical immunosensor to determine microcystin-LR in drinking water samples was developed. The assay was based on a non-competitive immuneassay. The electrochemical immunosensor allowed to determine the microcystin-LR at low concentration levels in drinking water samples. The immunosensor showed a very good analytical performance, with good reproducibility and a limit of detection of 33 pg mL^{-1} ($0.033 \text{ } \mu\text{g L}^{-1}$) which is well below the WHO guideline of $1 \text{ } \mu\text{g L}^{-1}$ good reproducibility. In addition, the ~~our~~ electrochemical immunosensor allows ~~has several advantages over other methods to determine microcystin-LR,~~ such as the direct measurement of the toxin without the use of a labeled hapten. All these characteristics make this device a promising tool to monitor microcystin-LR in water samples.

Acknowledgements

Financial supports from Agencia Nacional de Promoción Científica y Tecnológica (FONCYT) (PICT 0916/2010 and 270/2015), Ministerio de Ciencia y Tecnología de la Provincia de Córdoba (MINCyT) (Res. N°: 000109/2017), and Secretaría de Ciencia y Técnica (SECyT) (PPI 2016-2018, Res. 068/2016) from Universidad Nacional de Río Cuarto are gratefully acknowledged. Support was also obtained from CSIC, UdelaR, and ANII, Montevideo, Uruguay.

Micaela Boffadossi thanks to Universidad Nacional de Río Cuarto for a fellowship. Aylen Di Tocco thanks to CONICET for a doctoral research fellowship.

References

- [1] J. Wang (Ed.), *Analytical Electrochemistry*, 3rd ed., J. Wiley & Sons, Hoboken, New Jersey, USA, 2006.
- [2] W.I. Riberi, L.V. Tarditto, M.A. Zon, F.J. Arévalo, H. Fernández, Development of an electrochemical immunosensor to determine zearalenone in maize using carbon screen printed electrodes modified with multi-walled carbon nanotubes/polyethyleneimine dispersions, *Sens. Actuat. B-Chem.* 254 (2018) 1271–1277.
- [3] M. Iijima, S. Kuroda, Scaffolds for oriented and close-packed immobilization of immunoglobulins, *Biosens. Bioelectron.* 89 (2017) 810–821.
- [4] M. Park, Orientation control of the molecular recognition layer for improved sensitivity: a review, *BioChip J.* 13 (2019) 82-94.
- [5] S.S. Deshpande, 1996. *Enzyme immunoassays, from concept to product development.* Chapman & Hall, New York.

- [6] E. Barsoukov, J.R. MacDonald (Eds.), Impedance spectroscopy, theory, experiment and applications, third ed., J. Wiley & Sons, Hoboken, New Jersey, USA, 2018.
- [7] A.J. Bard, L.R. Faulkner (Eds.), Electrochemical methods. fundamentals and applications, second ed., J. Wiley & Sons, New York, 2000.
- [8] F. Ciucci, Modeling electrochemical impedance spectroscopy, *Current opinion in electrochemistry*, 13 (2019) 132-139.
- [9] J.S. Daniels, N. Pourmand, Label-free impedance biosensors: opportunities and challenges, *Electroanalysis* 19 (2007) 1239-1257.
- [10] Z. He, J. Wei, C. Gan, W. Liu, Y. Liu, A rolling circle amplification signal-enhanced immunosensor for ultrasensitive microcystin-LR detection based on a magnetic graphene-functionalized electrode, *RSC Adv.*, 7 (2017) 39906-39913.
- [11] D.R. de Figueiredo, U.M. Azeiteiro, S.M. Esteves, F.J. Goncalves, M.J. Pereira, Microcystin-producing blooms—a serious global public health issue, *Ecotoxicol. Environ. Saf.* 59 (2004) 151-163.
- [12] T.N. Duy, P.K.S. Lam, G.R. Shaw, D.W. Connell, Toxicology and risk assessment of freshwater cyanobacterial (blue-green algal) toxins in water, *Rev. Environ. Contam. Toxicol.* 163 (2000) 113-186.
- [13] R.E. Honkanen, J. Zwiller, R.E. Moore, S.L. Daily, B.S. Khatra, M. Dukelow, A.L. Boynton, Characterization of microcystin-LR, a potent inhibitor of type 1 and type 2A protein phosphatases, *J. Biol. Chem.* 265 (1990) 19401-19404.
- [14] Guidelines for drinking-water quality, 2nd ed. Addendum to Vol. 2. Health criteria and other supporting information. World Health Organization. WHO/SDE/WSH/03.04/57. Geneva, 1998.

- [15] L.G. Frenken, R.H. Van der Linden, P.W. Hermans, J.W. Bos, R.C. Ruuls, B. de Geus, C.T.J. Verrips, Isolation of antigen specific llama VHH antibody fragments and their high level secretion by *Saccharomyces cerevisiae*, *J. Biotechnol.* 78 (2000) 78 11-21.
- [16] R.C. Ladenson, D.L. Crimmins, Y. Landt, J.H. Ladenson, Isolation and characterization of a thermally stable recombinant anti-caffeine heavy-chain antibody fragment, *Anal. Chem.* 78 (2006) 4501-4508.
- [17] H.J. Kim, M.R. McCoy, Z. Majkova, J.E. Dechant, S.J. Gee, S. Tabares-da Rosa, G.G. Gonzalez-Sapienza, B.D. Hammock, Isolation of alpaca anti-hapten heavy chain single domain antibodies for development of sensitive immunoassay, *Anal. Chem.* 84 (2012) 1165-1171.
- [18] Macarena Pérez-Schirmer, Martín Rossotti, Natalia Badagian, Carmen Leizagoyen, Beatriz M. Brena, Gualberto Gonzalez-Sapienza, Comparison of Three Antihapten VHH Selection Strategies for the Development of Highly Sensitive Immunoassays for Microcystins, *Anal. Chem.* 2017, 89 6822-6806.
- [19] P. Chen, R.L. McCreery, Control of electron transfer kinetics at glassy carbon electrodes by specific surface modification, *Anal. Chem.* 68 (1996) 3958-3965.
- [20] X. Jia, Q. Xie, Y. Zhang, S. Yao, Simultaneous quartz crystal microbalance-electrochemical impedance spectroscopy study on the adsorption of anti-human immunoglobulin g and its immunoreaction at nanomaterial-modified Au electrode surfaces, *Anal. Sci.* 23 (2007) 689-696.
- [21] M.E. Orazem, B. Tribollet (Eds.), *Electrochemical impedance spectroscopy*, first ed., J. Wiley & Sons, Hoboken, New Jersey, USA, 2008.

- [22] A. Amano, T. Nakamura, S. Kimura, I. Morisaki, I. Nakagawa, S. Kawabata, S. Hamada, Molecular interactions of porphyromonas gingivalis fimbriae with host proteins: kinetic analyses based on surface plasmon resonance, *Infect. Immun.* 67 (1999) 2399-2405.
- [23] O.S. Wolfbeis (Series Ed.), J. Homola (Volume Ed.), Springer Series on chemical sensors and biosensors. surface plasmon resonance based sensors. Vol 4. Springer-Verlag Berlin Heidelberg, Germany. 2006.
- [24] J.P. Landry, Y. Ke, G.-L. Yu, X.D. Zhu, Measuring affinity constants of 1450 monoclonal antibodies to peptide targets with a microarray-based label-free assay platform, *J. Immunol. Methods* 417 (2015) 86–96.
- [25] ACS, Guidelines for data acquisition and data quality evaluation in environmental chemistry, *Anal. Chem.* 52 (1980) 2242-2249.
- [26] J. Wei, X. Xie, W. Chang, Z. Yang, Y. Liu, Ultrasensitive photoelectrochemical detection of microcystin-LR based on hybridization chain reaction assisted exciton-plasmon interaction and enzymatic biocatalytic precipitation, *Sens. Actuat. B-Chem.* 276 (2018) 180–188.
- [27] J. Wei, W. Chang, A. Qileng, W. Liu, Y. Zhang, S. Rong, H. Lei, Y. Liu, Dual-modal split-type immunosensor for sensitive detection of microcystin-LR: enzyme-induced photoelectrochemistry and colorimetry, *Anal. Chem.* 90 (2018) 9606-9613.
- [28] P. Pang, X. Teng, M. Chen, Y. Zhang, H. Wang, C. Yang, W. Yang, C.J. Barrow, Ultrasensitive enzyme-free electrochemical immunosensor for microcystin-LR using molybdenum disulfide/gold nanoclusters nanocomposites as platform and Au@Pt core-shell nanoparticles as signal enhancer, *Sens. Actuat. B-Chem.* 266 (2018) 400-407.

- [29] M. Barreiros dos Santos, R.B. Queirós, Á. Geraldes, C. Marques, V. Vilas-Boas, L. Dieguez, E. Paz, R. Ferreira, J. Morais, V. Vasconcelos, J. Piteira, P.P. Freitas, B. Espiña, Portable sensing system based on electrochemical impedance spectroscopy for the simultaneous quantification of free and total microcystin-LR in freshwaters, *Biosens. Bioelectron.* 142 (2019) 111550.
- [30] T. Guan, W. Huang, N. Xu, Z. Xu, L. Jiang, M. Li, X. Wei, Y. Liu, X. Shen, X. Li, C. Yi, H. Lei, Point-of-need detection of microcystin-LR using a smartphone-controlled electrochemical analyzer, *Sens. Actuat. B-Chem.* 294 (2019) 132-140.
- [31] M. Li, S.K. Paidi, E. Sakowski, S. Preheim, I. Barman, Ultrasensitive detection of hepatotoxic microcystin production from cyanobacteria using surface-enhanced raman scattering immunosensor, *ACS Sens.* 4 (2019) 1203-1210.
- [32] W. Liu, C. Gan, W. Chang, A. Qileng, H. Lei, Y. Liu, Double-integrated mimic enzymes for the visual screening of microcystin-LR: copper hydroxide nanozyme and G-quadruplex/hemin DNAzyme, *Anal. Chim. Acta* 1054 (2019) 128-136.
- [33] Z. He, Y. Cai, Z. Yang, P. Li, H. Lei, W. Liu, Y. Liu, A dual-signal readout enzyme-free immunosensor based on hybridization chain reaction-assisted formation of copper nanoparticles for the detection of microcystin-LR, *Biosens. Bioelectron.* 126 (2019) 151–159.
- [34] J. Qin, X. Sun, D. Li, G. Yan, Phosphorescent immunosensor for simple and sensitive detection of microcystin-LR in water, *RSC Adv.* 9 (2019) 12747–12754.

Figure Captions

Scheme 1. Schematic representation of the electrochemical immunosensor to determine microcystin-LR Nab A2/streptavidin/GC electrode.

Figure 1. Equivalent circuit used to fit the impedance spectra. All components of the circuit are defined in the text.

Figure 2. Cyclic voltammograms of $1 \times 10^{-3} \text{ mol L}^{-1} \text{ Fe}(\text{NH}_4)_2(\text{SO}_4)_2 + 0.1 \text{ mol L}^{-1} \text{ KCl}$ solution for polished CG electrode (A) and after oxidation in $0.1 \text{ mol L}^{-1} \text{ H}_2\text{SO}_4$ (B) acid and basic $0.1 \text{ mol L}^{-1} \text{ NaOH}$ (C) solutions. media.

Figure 3. Complex impedance plots (Nyquist diagrams) obtained for □) GC electrode and ○) streptavidin/GC electrode. Streptavidin concentration was $100 \mu\text{g mL}^{-1}$. The solid lines correspond to the fit of the experimental points using the electrical circuit described in Fig. 1. A $2 \times 10^{-3} \text{ mol L}^{-1} [\text{Fe}(\text{CN})_6]^{-4/-3} + 0.1 \text{ mol L}^{-1} \text{ KCL}$ solution was used.

Figure 4. Electrochemical impedance spectra obtained for biotin-Nab concentrations of: □) 2.5, ○) 5, ◇) 10 and Δ) $15 \mu\text{g mL}^{-1}$. The solid lines correspond to the fit of the experimental points. A $2 \times 10^{-3} \text{ mol L}^{-1} [\text{Fe}(\text{CN})_6]^{-4/-3} + 0.1 \text{ mol L}^{-1} \text{ KCL}$ solution was used.

Figure 5. Variation of Z as a function of time for microcystin-LR concentrations. a) 0, b) 0.01, c) 0.1, d) 1 and e) 10 ng mL^{-1} . All impedimetric sensograms were performed at a frequency of 80 Hz. Insert plot: saturation curve obtained for microcystin-LR using the electrochemical immunosensor. A $2 \times 10^{-3} \text{ mol L}^{-1} [\text{Fe}(\text{CN})_6]^{-4/-3} + \text{PBS}$ solution was used.

Figure 6. Plots of $\partial Z/\partial t$ vs. Z for different microcystin-LR concentrations. The dots represent the experimental data, and the dashed line represents the fit of the experimental data.

Figure 7. Kinetic analysis of microcystin-LR bonded to Nab A2. The slopes obtained from the $\partial Z/\partial t$ vs. Z for each impedimetric sensogram were plotted vs. the microcystin-LR concentration. Each point is the average of three replicated measurements.

Figure 8. Calibration curve obtained for the quantification of microcystin-LR. Each point is the average of four replicated measurements. The statistic parameters obtained for the curve are $R^2 = 0.9906$ and $\chi^2 = 1.05 \times 10^{-3}$. Insert of the Figure shows the electrochemical impedance spectra recorded for microcystin-LR concentrations of 0, 1×10^{-3} , 1×10^{-2} , 1×10^{-1} , 1, 10 y 100 ng mL^{-1} . A $2 \times 10^{-3} \text{ mol L}^{-1} [\text{Fe}(\text{CN})_6]^{4-/3-} + 0.1 \text{ mol L}^{-1} \text{ KCL}$ solution was used. The arrow shows the increase in the concentration of microcystin-LR.

Table 1. Reproducibility of the electrochemical immunoassay for the microcystin-LR determination.

Microcystin-LR concentration ng mL ⁻¹	Inter-assay		
	Mean (ohm)	Standard deviation (ohm)	%CV
0.1	1057	52	5
1	1349	41	3
10	1938	36	2

Table 2. Different methods proposed to quantify microcystin-LR in water samples.

Class of immunosensor	Linear range / ng L⁻¹	LOD / ng L⁻¹	Year	Ref.
Photoelectrochemical immunosensor	0.5 to 1x10 ²	0.3	2018	[26]
Photoelectrochemical immunosensor	5x10 ⁻² to 5x10 ³	0.03	2018	[27]
Electrochemical immunosensor using DPV	1.0 to 1x10 ⁶	0.3	2018	[28]
Electrochemical immunosensor using EIS	1x10 ² to 3.3x10 ⁵	0.57	2019	[29]
Amperometric immunosensor	1 to 1x10 ⁵	0.11	2019	[30]
SRC immunosensor	10 to 1x10 ⁵	14	2019	[31]
Optical immunosensor	7 to 7.5x10 ⁴	6	2019	[32]
Electrochemical immunosensor using DPV	5 to 2x10 ⁴	2.8	2019	[33]
Phosphorescent immunosensor	2x10 ² to 2x10 ⁴	24	2019	[34]
Electrochemical immunosensor using EIS	1 x10 ² to 1x10 ⁴	33	2020	Our work

DPV: differential pulse voltammetry

SRC: surface-enhanced Raman scattering

Table 3. Reproducibility of electrochemical immunosensor for the determination of microcystin-LR in drinking water samples.

Water reservoir	Microcystin-LR concentration / ng mL ⁻¹	R _{ct} / ohm	Mean / ng mL ⁻¹	Recovery
Center zone	0.1	763	0.091±0.007	91 %
	1	1350	1.21±0.01	121 %
North zone	0.1	759	0.085±0.008	85 %
	1	1385	1.28±0.05	128 %
South zone	0.1	802	0.116±0.009	116 %
	1	1290	0.88±0.07	88 %
East zone	0.1	749	0.082±0.003	82 %
	1	1310	1.03±0.05	103 %

Figure 1

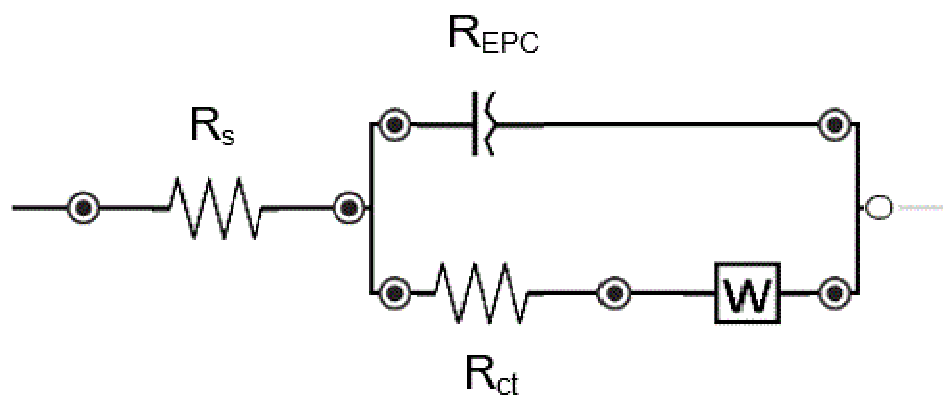


Figure 2

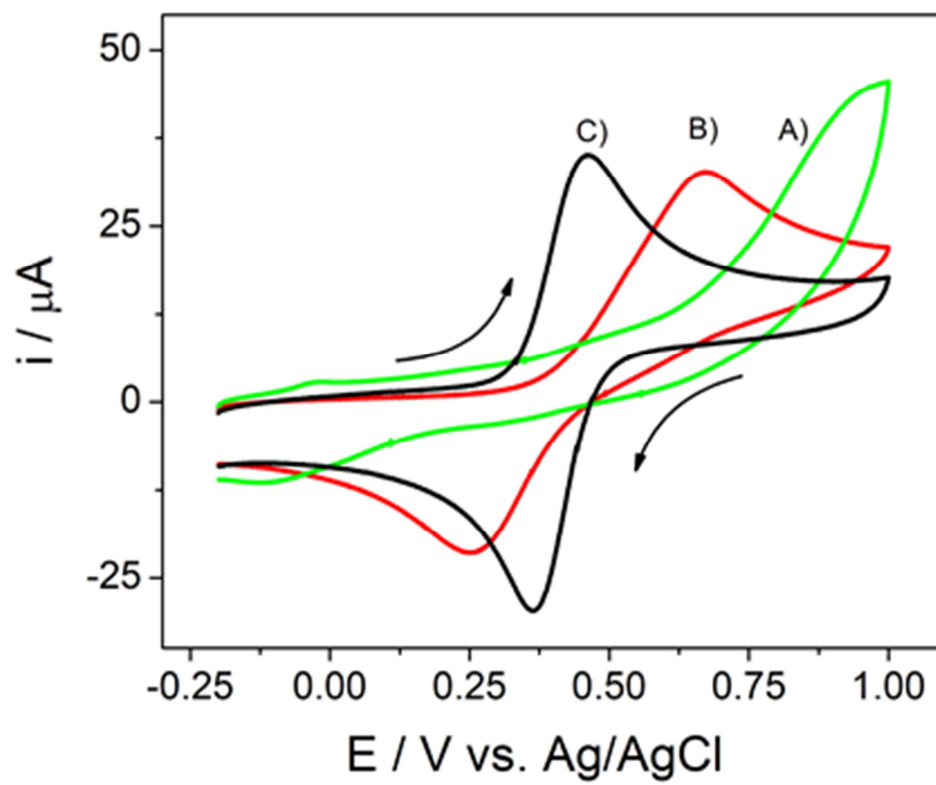


Figure 3

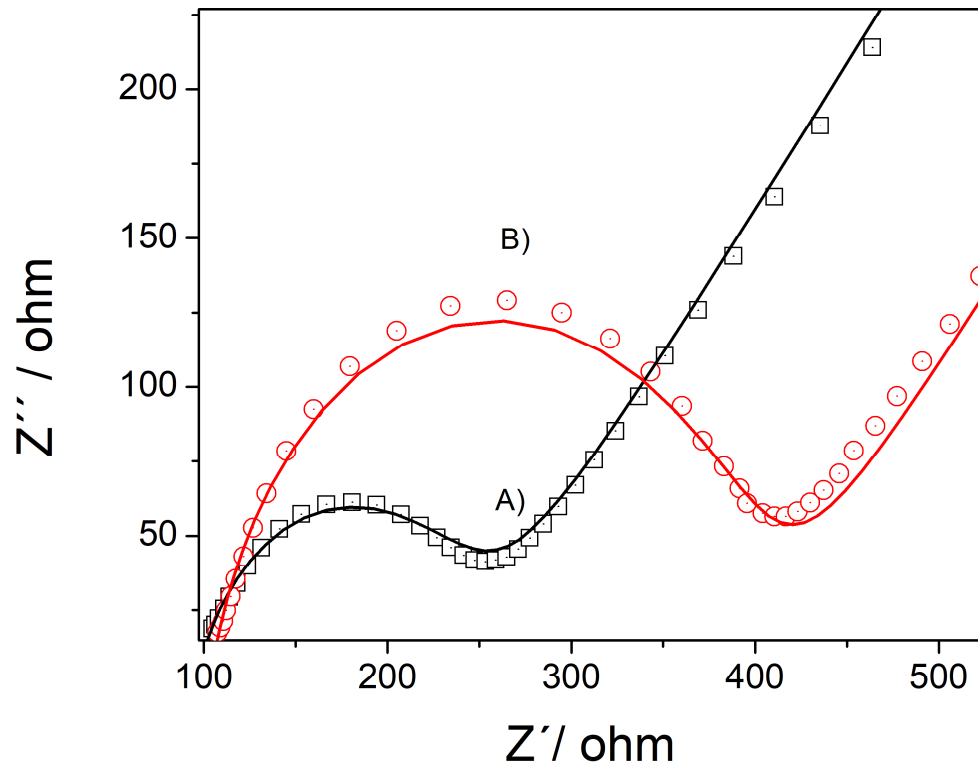


Figure 4

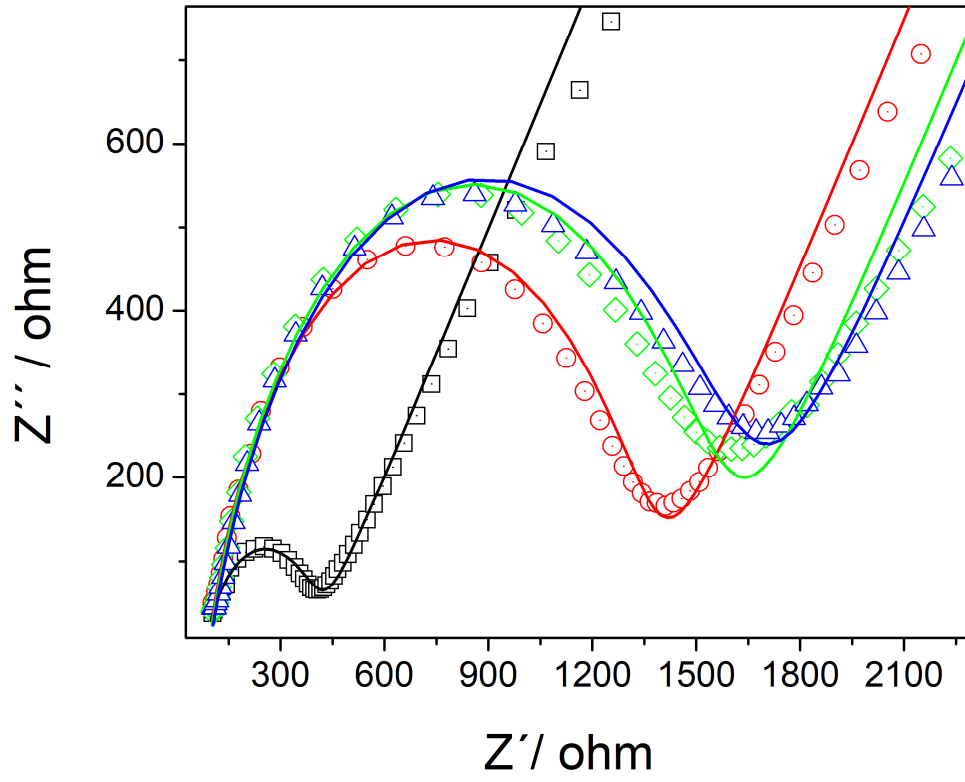


Figure 5

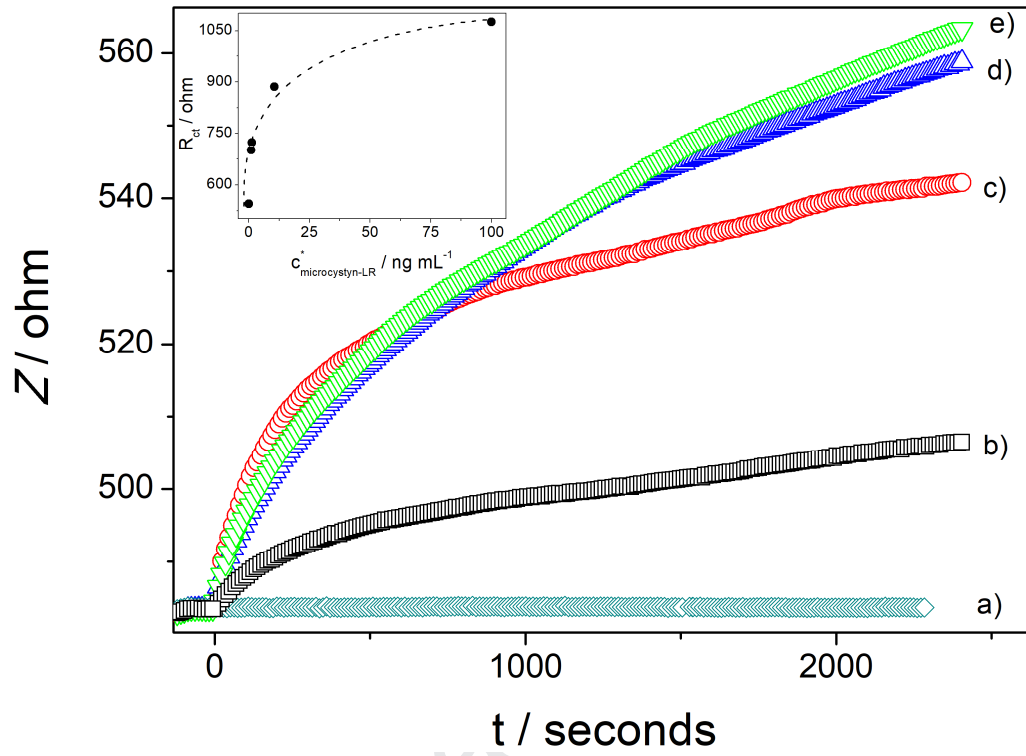


Figure 6

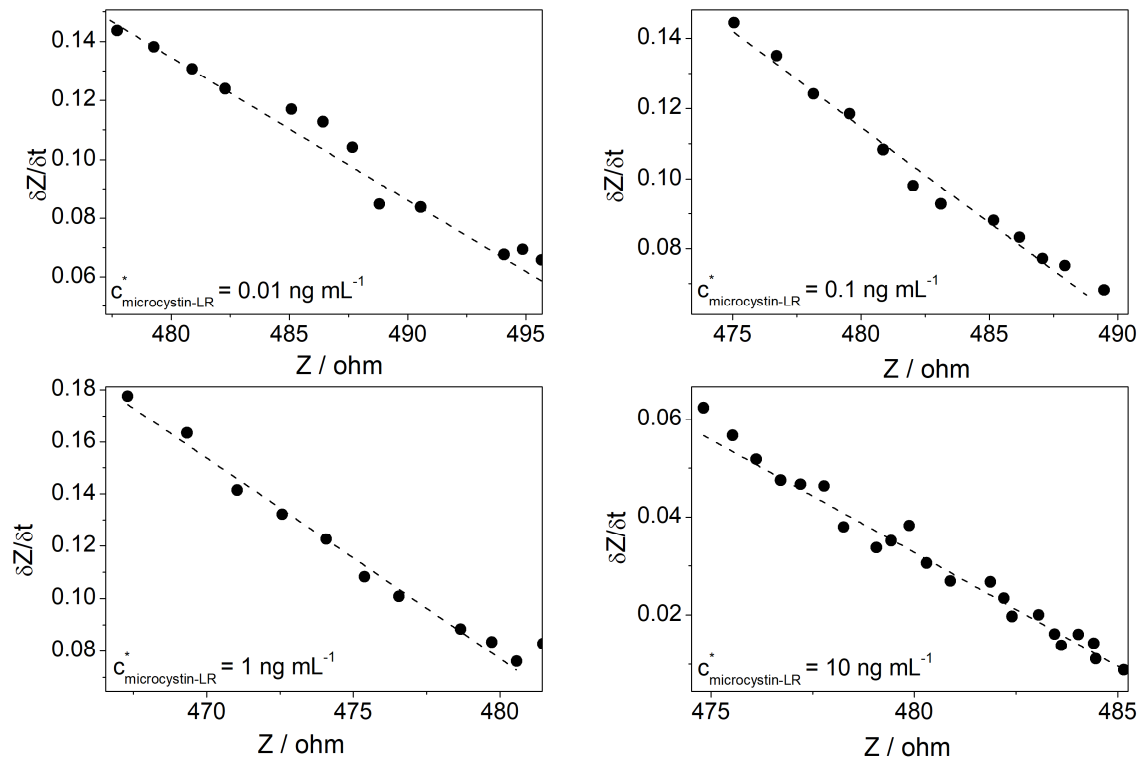


Figure 7

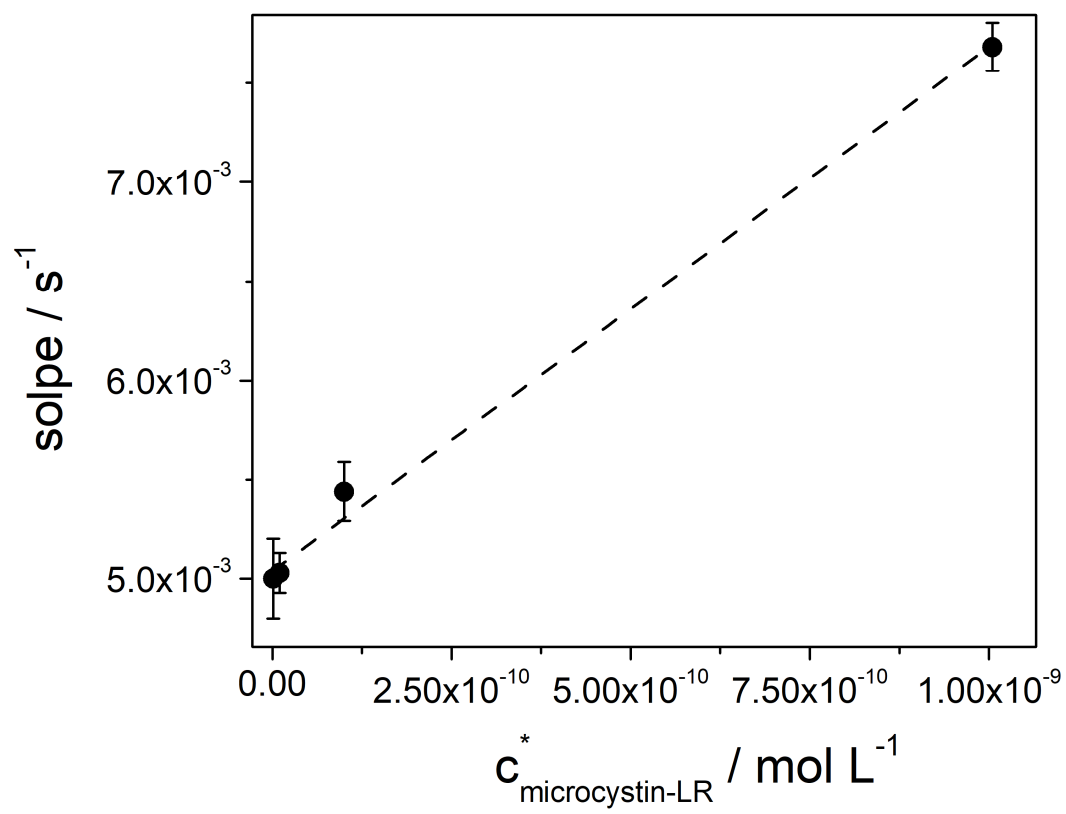
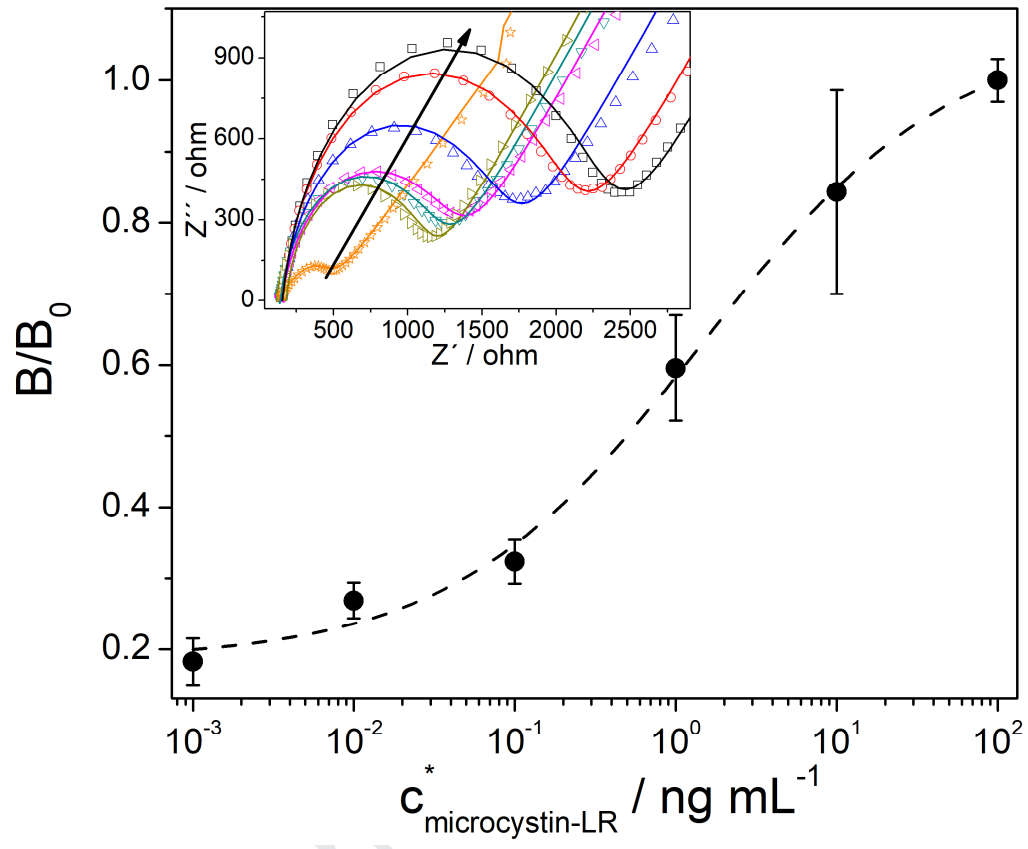
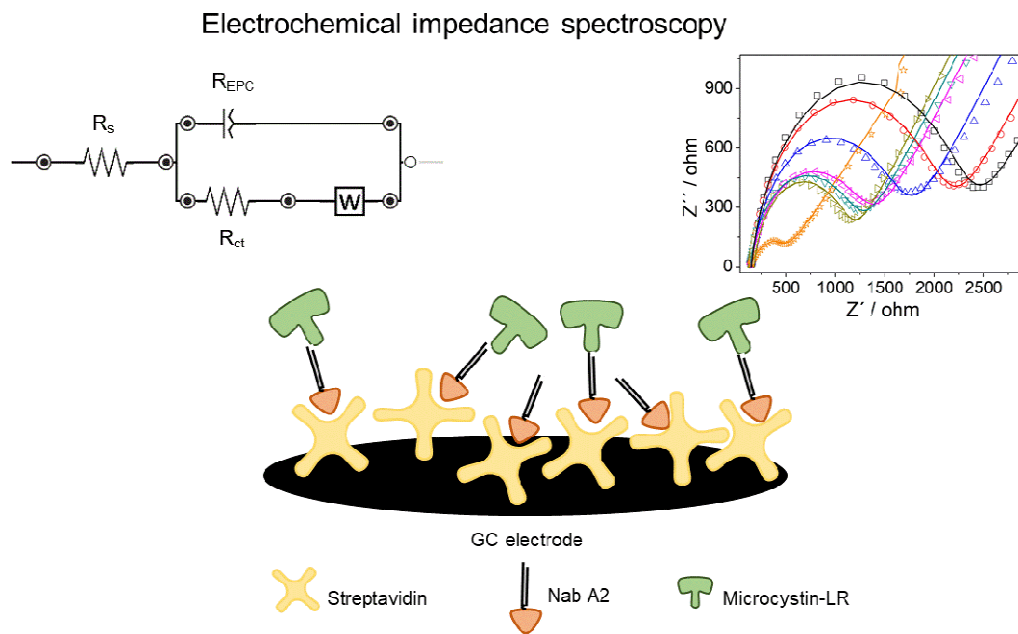


Figure 8



Scheme 1



Declaration of interests

The authors declare that they have no known competing financial interests or personal relationships that could have appeared to influence the work reported in this paper.

The authors declare the following financial interests/personal relationships which may be considered as potential competing interests:

There are no financial interests / personal relationships for all authors presents in this work

Journal Pre-proof